ELSEVIER

Journal of Power Sources 81–82 (1999) 925–929

JOURNAL OF POWER SOURCES

www.elsevier.com/locate/jpowsour

Dendritic growth mechanisms in lithium/polymer cells

C. Brissot [a], M. Rosso [a,*], J.-N. Chazalviel [a], S. Lascaud [b]

[a] *Laboratoire de Physique de la Matière Condensée, Ecole Polytechnique, CNRS, 91128 Palaiseau, France*
[b] *EDF / DER, BP 1, 77250, Moret sur Loing, France*

Abstract

Direct in situ observation of dendritic electrodeposition of lithium has been performed in symmetrical lithium/PEO-LiTFSI cells under galvanostatic conditions. Our experimental set-up allows us to measure simultaneously the variation of the cell potential, the evolution of the dendrites, and the variation of the ionic concentration in the electrolyte around the dendrites. Depending on current density, we observe two different regimes for the dendritic growth: at high current density, dendrites start when the ionic concentrations drop to zero at the negative electrode, whereas at low current density, local inhomogeneities seem to play a major role.

Keywords: In situ visualisation; Dendrites; Lithium; Polymer electrolyte; Batteries

1. Introduction

The market for secondary batteries is growing very fast, thanks to the development of new applications encompassing such fields as games, consumer electronics, cellular communications, transportation, portable computers, electric vehicles… Among these batteries, the lithium/polymer battery has specific advantages: indeed, this technology, which was introduced by Armand et al. [1,2] several years ago, is characterized by the low weight and the high specific capacity of the battery and also solid state, adhesiveness and elastomericity of the electrolyte. In particular, these electrolyte properties make them easy to manufacture by film process. Another advantage is that, compared with liquid electrolyte, lithium/polymer batteries tend to develop less dendrites. Nonetheless, the formation of dendrites remains a problem for the charge efficiency of this battery. Our aim is to understand the dendritic growth mechanism in order to prevent or to limit this phenomenon.

2. Experimental conditions

Direct in situ observation of dendritic electrodeposition of lithium [3] has been performed in symmetrical lithium/polymer cells under galvanostatic conditions at a temperature of 80°C. The polymer electrolyte consists of poly(ethylene oxide) ($Mw = 3.10^5$) and of the lithium salt $LiN(CF_3SO_2)_2$ (abbreviated in LiTFSI), discovered by Armand et al. [1,2]. The salt concentration in terms of O/Li ratio is in the range 15–40. The electrolyte is prepared in an argon-filled dry box. The polymer and the salt are mixed with acetone and acetonitrile: the mixture is heated until it becomes homogeneous. After having removed bubbles under vacuum, the electrolyte is spread on a spin-coating machine and dried to remove the solvents. The obtained films are about 100 μm thick. Superposition of several layers is then needed to obtain a film compatible with the thickness of the lithium electrodes (160 or 380 μm). The distance between the two lithium electrodes is about 1 mm. External contacts are nickel collectors, connected to a standard electrochemical set-up (Schlumberger 1286 interface and Solartron 1250 frequency response analyser).

Our experimental set-up (Fig. 1) allows us to observe gradient concentration maps in the cells [4] and simultaneously to follow the evolution of the potential with time. We have studied the evolution of dendrites from the onset

* Corresponding author

0378-7753/99/$ - see front matter
PII: S0378-7753(98)00242-0

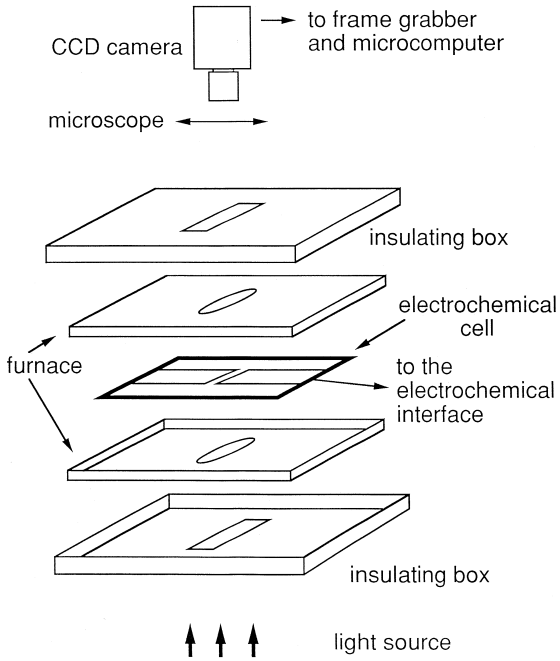

Fig. 1. Schematic view of the experimental set-up.

to the end of the growth. The dendritic growth was recorded with a microscope and a CCD camera and the pictures were analysed with National Institute of Health (NIH) Image processing software.

3. Results

3.1. Two electrochemical regimes

The evolution of ionic concentrations C_a and C_c in a binary electrolyte submitted to a constant current density may be described by the following set of equations [5]:

$$\frac{\partial C_c}{\partial t} = D_c \frac{\partial^2 C_c}{\partial x^2} + \mu_c \frac{\partial}{\partial x}\left(C_c \frac{\partial V}{\partial x}\right) \quad (1)$$

$$\frac{\partial C_a}{\partial t} = D_a \frac{\partial^2 C_a}{\partial x^2} - \mu_a \frac{\partial}{\partial x}\left(C_a \frac{\partial V}{\partial x}\right) \quad (2)$$

where subscripts c and a refer to cation and anion, respectively, D refers to the diffusion constants, μ to mobilities and V is the electrostatic potential. For this set of equations to be valid, it is necessary that the diffusion constants and mobilities are independent of concentration. This is certainly not true in our system [3,6] but this approximation allows us to give a simple description of its behaviour.

Supposing $z_a C_a \approx z_c C_c \approx C$, the system becomes:

$$\frac{\partial C}{\partial t} = D_c \frac{\partial^2 C}{\partial x^2} + \mu_c \frac{\partial}{\partial x}\left(C \frac{\partial V}{\partial x}\right) \quad (3)$$

$$\frac{\partial C}{\partial t} = D_a \frac{\partial^2 C}{\partial x^2} - \mu_a \frac{\partial}{\partial x}\left(C \frac{\partial V}{\partial x}\right) \quad (4)$$

z_a and z_c are the anionic and cationic charge numbers, respectively. Elimination of the potential-dependent term leads to a simple ambipolar diffusion equation:

$$\frac{\partial C}{\partial t} = D \frac{\partial^2 C}{\partial x^2} \text{ with } D = \frac{D_a \mu_c + D_c \mu_a}{\mu_c + \mu_a} \quad (5)$$

At the electrodes the current density is entirely due to cations ($J = J_c$ and $J_a = 0$), hence:

$$-D_c \frac{dC_c}{dx} - \mu_c C_c \frac{dV}{dx} = \frac{J}{z_c e} \quad \text{for } x = 0 \quad (6)$$

$$-D_a \frac{dC_a}{dx} + \mu_a C_a \frac{dV}{dx} = 0 \quad \text{for } x = 0 \quad (7)$$

where e is the elementary charge.

Here again, the elimination of the V-dependent term yields, as the boundary condition:

$$\frac{\partial C}{\partial x}(x = 0) = \frac{-J}{eD\left(1 + \frac{\mu_c}{\mu_a}\right)} \quad (8)$$

From this equation, one can predict two different behaviours for a symmetrical cell, depending on the inter electrode distance L, the initial concentration C_0, the diffusion constant D, and the current density J (see Fig. 2).

(a) If $dC/dx < 2C_0/L$, the ionic concentration profile evolves to a steady state (see Fig. 2a) where the concentration gradient is constant [7]. The potential also attains a stationary value.

(b) If $dC/dx > 2C_0/L$, the concentration will go to zero at the negative electrode at a time τ, called the 'Sand's time'. At this time, the potential will eventually diverge (see Fig. 2b). In practice, in this regime the distance L is larger than the diffusion length $\ell = \sqrt{D\tau}$ at the time τ: this is the so-called 'semi-infinite approximation' [4]. Solving Eq. (5) with the boundary condition (8) leads to a simple expression for τ:

$$\tau = \pi D\left(\frac{C_0 e}{2Jt_a}\right)^2 \text{ with } t_a = \frac{\mu_a}{\mu_a + \mu_c} \quad (9)$$

t_a is the anionic transport number.

From Eq. (8), we notice that dC/dx linearly depends on J. For a given distance L between the electrodes, behaviours (a) and (b) will be found at low and high J, respectively. The crossover value J^* is given by:

$$J^* = \frac{2eC_0 D}{t_a L} \quad (10)$$

Fig. 2a and b show typical potential variations in the two above-mentioned cases. In these experiments, the ini-

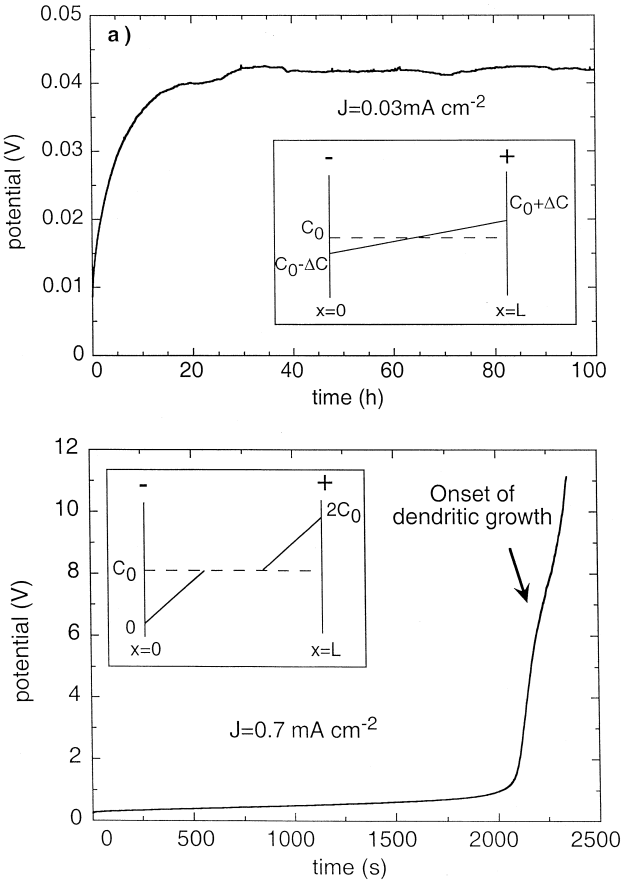

Fig. 2. For a given distance L between the electrodes, (a) if $J < J^*$, the system evolves to a steady state where the concentration varies linearly from $C_0 - \Delta C$ at the negative electrode to $C_0 + \Delta C$ at the positive electrode, (b) if $J > J^*$ (semi-infinite approximation), the ionic concentration drops to zero and the cell potential diverges at the Sand's time. Here, the Sand's time is about 2100 s (note the different time scales in (a) and (b). The inflexion on the $V(t)$ curve shown by the arrow corresponds to the onset of dendritic growth.

tial concentration is $O/Li = 20$ ($C = 6 \times 10^{20}$ cm^{-3}), the inter electrode distance is 1.2 mm, supposing a cationic transport number t_c of 0.2, and a diffusion constant of 9×10^{-8} cm^2 s^{-1}, this gives $J^* = 0.18$ mA cm^{-2}.

3.2. Dendritic growth

Our experimental set-up permits to observe dendritic growth in a large range of current densities. In the two above-mentioned regimes, we will mainly describe the onset, the evolution of dendritic growth and the morphology of dendrites.

3.2.1. The high current–density regime

We generally do not observe dendrites during the very first polarization of a cell (we must recall that because of the divergence of the potential at τ, the duration of the polarization is limited). Dendrites only appear after a few cycles, usually when the potential starts diverging (see Fig. 2b). Accordingly, the time variation of the potential observed at τ becomes much slower than during the first polarization. We observe that (i) the dendrites have arborescent-like morphologies (Fig. 3) and that (ii) they seem to be unable to grow beyond a given distance of the electrode [3].

In the high current–density regime, the onset of the growth and the growth itself are understood in the framework of Fleury et al. [8,9], Chazalviel et al. [10] and Rosso et al.'s [11] model: in this regime, the ionic concentrations in the vicinity of the negative electrode drop to zero at the Sand's time. However, a different behaviour occurs for the anionic and the cationic concentrations leading to an excess of positive charges at the negative electrode. This results in a local space charge associated with a large electric field. This situation creates instabilities such as dendritic growth [12]. This model then predicts that dendrites appear at a time very close to the Sand's time τ.

Moreover, Chazalviel's model predicts that, in order to avoid the increase of the space charge, dendrites must grow at a velocity equal to the drift velocity $-\mu_a E_0$ of the anions in the applied electric field E_0, where $E_0 = J/\sigma$ and σ is the conductivity of the electrolyte. Our experiments confirm this prediction. Indeed, we observe that dendrites usually grow at a constant velocity, very close to the velocity at which the anions withdraw from the working electrode. Also, we have measured concentration gradients by an optical method [4]: the result is shown in Fig. 3. Because of the concentration gradient in the vicinity of the electrode there is an optical index variation which deviates parallel incident light: this results in a lighter region in front of the dendrites, which evidences this gradient. We have observed that this depleted zone ahead of the dendrites remains almost the same during the growth.

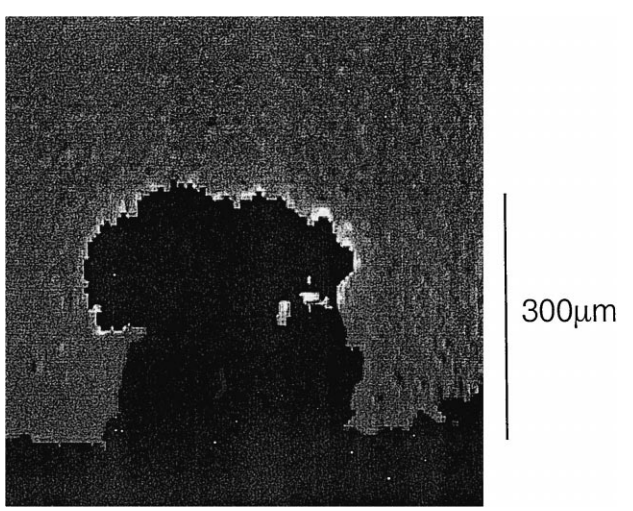

Fig. 3. At high current densities (here $J = 0.7$ mA cm^{-2}) the dendrites have an arborescent like morphology. Variations of light intensity (white color) seen at the top of the growing dendrite, are due to index gradients, evidencing concentration variations in the electrolyte.

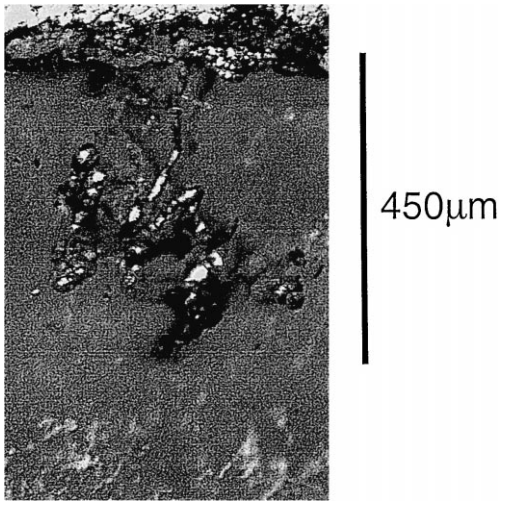

Fig. 4. Photograph of a dendrite obtained in the low-density regime: $J = 0.1$ mA cm^{-2}. This picture has been taken after the experiments, at room temperature.

However, after a few cycles, one observes that the dendritic growth is enhanced by cycling: dendrites can start growing soon after the beginning of the polarization; and large fluctuations of the dendrite velocity appear [3], that we attribute to current–density inhomogeneities along the electrode due to the enhancement of local inhomogeneities by cycling.

3.2.2. The low current–density regime

Contrarily to the high current–density regime, the concentration does not go to zero at the negative electrode. At very low current density, the concentration even remains very close to C_0 throughout the cell [this point has been confirmed experimentally, see Refs. [13,14]]: however, we observe dendrites. In this regime, the duration of a polarization is not limited by the divergence of the cell potential: this allows us to polarize the cell until dendrites appear and eventually short-circuit the cell. We observe that dendrites start growing after a time which increases when the current density decreases (typically, this time may be of the order of several hours for a current density of 0.1 mA cm^{-2}): the reason for this dependence is not fully understood at present.

The dendrites have needle-like morphologies very similar to those reported in the literature [15,16]: as shown in Fig. 4, they appear as bright, metallic filaments. Their cross section is about 10–20 μm which makes them very fragile: motions in the bulk of the electrolyte [3] tend to break the dendrites so that they cannot participate in the electrochemical process during the following reverse polarizations. The dendrites can either grow straight to the positive electrode and short-circuit the cell (Fig. 5a) or grow in a tortuous way and never induce a short-circuit. When dendrites start growing the potential starts decreasing (Fig. 5b). This is due to the fact that while the dendrites go towards the positive electrode, the effective inter electrode distance is decreased, hence, the potential drops.

In this regime, concentration gradients are much lower than in the high current–density regime. As a consequence we are not able to observe these gradients by the optical technique mentioned above.

Finally, we observe that, as in the high current–density regime, the growth velocity is in agreement with Chazalviel's model, i.e., $v = \mu_a E_0$.

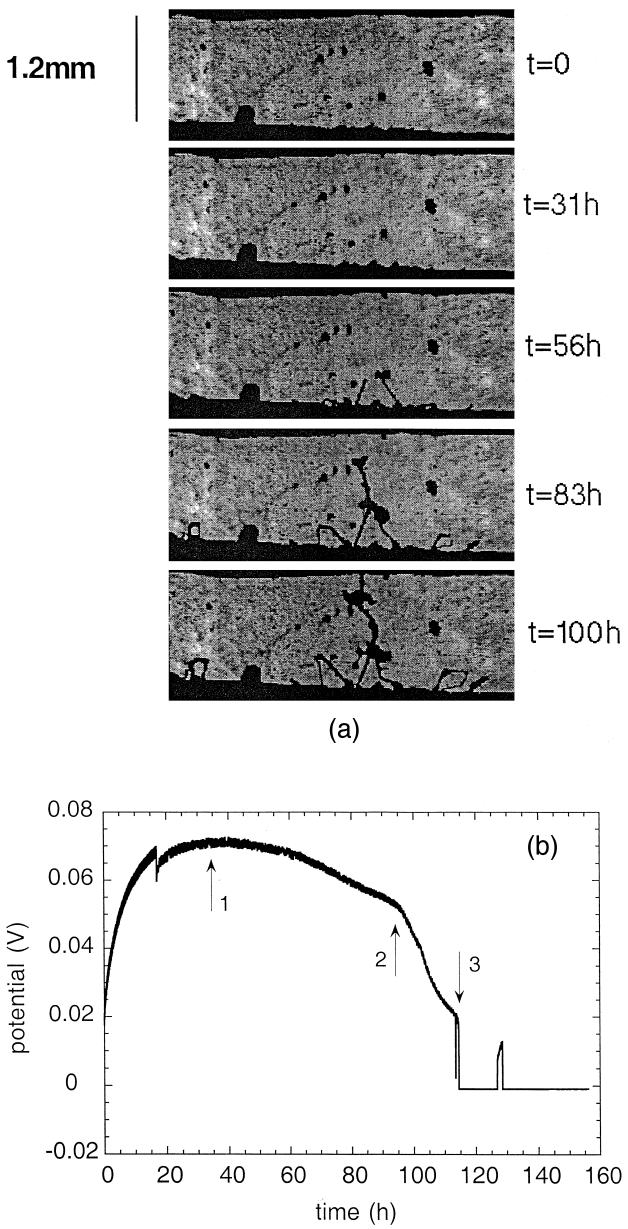

Fig. 5. Time variation of the dendrites observed in the inter-electrode space while polarizing the cell with $J = 0.05$ mA cm^{-2}. (a) Dendrites are seen to be needle-like. (b) The evolution of the cell potential reflects the evolution of the dendrites: arrow 1 ($t \sim 38$ h) corresponds to the onset of the growth, whereas arrow 2 ($t \sim 100$ h), shows the time when the largest dendrite contacts the positive electrode. Finally, this dendrite short-circuits the cell (arrow 3). Note: the potential jump seen at $t = 17$ h corresponds to a short interruption of the polarization.

Note: Our cells have a geometry which is very far from that of actual batteries. In order to check that our results do not depend on this specific geometry, we have also performed experiments in cells having a geometry close to the geometry of batteries: in this case, the cells essentially consist of two lithium foils sandwiching a polymer electrolyte layer about 100 μm thick. These cells do not permit direct in situ visualisation of the dendrites. We have also investigated the two above-mentioned regimes (here $J^* \sim 2$ mA cm^{-2}). In particular, in the high current–density regime, during the first polarization, we do not detect anomalies on the time variation of the potential which could be related to the onset of dendritic growth: such anomalies only appear after cycling the cells, in agreement with what is observed in our cells. Also, in the low current–density regime, one observes sudden decreases in the $V(t)$ curves, very similar to those shown in Fig. 5.

4. Conclusion

We have compared the dendritic growth in two electrochemical regimes, i.e., at low and at high current density. In the high current–density regime, we do not see dendrites during the very first polarization. However, when cycling the cell, dendrites appear, first at the Sand's time, then earlier and earlier during subsequent polarizations, probably due to local defects. The onset of the growth (first polarizations) and the growth velocity of the dendrites are in agreement with the prediction of Chazalviel's model.

In the low current–density regime, where the concentration variations can be very weak, we also observe dendrites, but with a very different morphology. In this case, it seems that one cannot explain the onset of the growth in the framework of Chazalviel's model. However, the growth velocity agrees with Chazalviel's model. We believe that this apparent contradiction might be due to the existence and/or formation of local inhomogeneities at the surface of the electrode (related either to the geometry of the electrode or to the passivation layer). This could also explain the formation of dendrites which is observed, much before the Sand's time, after cycling the cell in the high current–density regime.

References

[1] M. Armand, J.M. Chabagno, M.J. Duclot, in: P. Vashishta (Ed.), Fast Transport in Solids, North-Holland, New York, 1979, p. 131.
[2] M. Armand, W. Gorecki, R. Andréani, in: B. Scrosati (Ed.), Second Int. Symp. on Polymer Electrolytes, Elsevier, London, 1990, p. 91.
[3] C. Brissot, M. Rosso, J.-N. Chazalviel, P. Baudry, S. Lascaud, Electrochim. Acta 43 (1998) 1569.
[4] C. Brissot, M. Rosso, J.-N. Chazalviel, S. Lascaud, to be published.
[5] A.J. Bard, L.R. Faulkner, Electrochemical Methods. Fundamentals and Applications, Wiley, 1980.
[6] S. Lascaud, PhD Thesis, University of Montréal, 1996.
[7] P.G. Bruce, C.A. Vincent, J. Electroanal. Chem. 225 (1987) 1.
[8] V. Fleury, J.-N. Chazalviel, M. Rosso, Phys. Rev. Lett. 68 (1992) 2492.
[9] V. Fleury, J.-N. Chazalviel, M. Rosso, Phys. Rev. E 48 (1993) 1279.
[10] J.-N. Chazalviel, V. Fleury, M. Rosso, in: Council of Scientific Research Integration (Ed.), Trends in Electrochemistry, Research Trends, India, 1992, p. 231.
[11] M. Rosso, J.-N. Chazalviel, V. Fleury, E. Chassaing, Electrochim. Acta 39 (1994) 507.
[12] J.-N. Chazalviel, Phys. Rev. A 42 (1990) 7355.
[13] I. Rey, Thesis, University of Bordeaux I, 1997.
[14] I. Rey, J.-L. Bruneel, J. Grondin, L. Servant, J.-C. Lassègues, to be published.
[15] I. Yoshimatsu, H. Toshiro, J. Yamaki, J. Electrochem. Soc. 135 (1988) 2422.
[16] M. Arakawa, S. Tobishima, Y. Nemoto, M. Ichimura, J. Yamaki, J. Power Sources 43–44 (1993) 27.